

Photochemistry

Photoredox Autocatalysis: Towards a Library of Generally Applicable Sulfonamide Reductive Photocatalysts

Jaspreet Kaur⁺, Mark John P. Mandigma⁺, Nakul Abhay Bapat, and Joshua P. Barham*

Abstract: Dichotomous thinking dominates the field of synthetic photochemistry—either a reaction needs a photocatalyst or not. Herein, we report the identification of a photoredox autocatalytic pathway - an alternative to the existing mechanistic paradigms - to access cyclic biaryl sulfonamides (BASNs). This reaction does not require exogenous catalyst as the visible light absorbing deprotonated product - with potent excited state reductive power - acts as the photocatalyst for its own synthesis. This finding implicated BASN as a novel organophotocatalyst architecture and allowed a rapid, modular, and low-cost combinatorial synthesis of a BASN library that expedited optimal photocatalyst screening. Furthermore, BASN was revealed as a widely applicable organophotocatalyst for diverse transition metal-free transformations such as: intramolecular (spiro)-cyclizations, defunctionalizations, and C–C / C-heteroatom couplings.

photoredox catalysis; where a catalytic chromophore is used to harvest energy from light to induce SET events^[2] and ii) photocatalyst-free reactions; such as irradiation of visible light absorbing substrates or electron donor-acceptor (EDA) complexes^[3] generally involving stoichiometric reactants (Figure 1A, left). Both have their own advantages and drawbacks. For example, the former strategy enjoys the redox activation of non-photo absorbing substrates but requires an initial effort of screening appropriate photocatalysts which are often expensive or can require elaborate synthesis. On the other hand, the latter strategy boasts a green and cost-effective alternative (as it is photocatalyst-free) but requires reactants to either be sufficiently photo-absorbing or electronically biased such that they form photo-absorbing complexes. There is a process with intermediary characteristics of the two, whereby no external photocatalyst is needed at the start of the reaction but as the product accumulates, the reaction accelerates.^[4,5] The third process, called photoredox autocatalysis, inherits the assets of the aforementioned popular pathways by using an intermediate or product as the photocatalyst for its own formation (Figure 1A, right).

Introduction

The use of visible light to drive chemical reactions has been one of the most successful contemporary advances in organic synthesis. Notably, it has allowed redox and radical chemistries to flourish and paved ways to rapidly access molecular complexities by open-shell mechanisms that are rather difficult to achieve otherwise.^[1] Accessing radical intermediates by photo-induced single electron transfer (SET) is mostly dominated by two popular strategies: i)

Autocatalysis is an important process found in biochemical pathways and is often attributed as the primordial method for amplification of homochirality in the origins of life.^[6] It has been observed in various thermal reactions such as Soai reaction^[7] and others.^[8] Auto-photocatalysis^[9–11] has limited examples in synthetic photochemistry which so far relate to net-oxidative processes, including i) a Chan–Lam coupling where the ligation of product imparted photocatalytic ability to a copper complex,^[9] and ii) autocatalytic photosensitized oxidation of naphthols to naphthoquinones^[11] (Figure 1A, right). Auto-photocatalytic pathways that proceed purely by SET redox processes, are net-redox-neutral, and/or that involve cheap, diversifiable organic catalysts (organo-auto-PRC), are yet to be explored in synthetic chemistry. However, such pathways represent exciting frontiers in synthetic photochemistry, with the potential to illuminate unexplored reactivities.

In recent years, organophotocatalysts have proven to be viable alternatives to traditional precious transition metal photocatalysts, offering ease of preparation, sustainability, as well as desirable photophysical and redox properties.^[12] Inspired by the prominence of sulfonamides in medicinal chemistry, due to their rigidity and exceptional chemical/metabolic stability, we reasoned that sulfonamide containing moieties would be good candidates for inexpensive, and stable photocatalyst frameworks. Interestingly, the sulfonamide functionality in photocatalyst structure is unprece-

[*] J. Kaur,⁺ N. A. Bapat, J. P. Barham
 Institute of Organic Chemistry
 University of Regensburg, Universitätsstr. 31, Regensburg, 93053,
 Germany
 E-mail: Joshua-Philip.Barham@chemie.uni-regensburg.de

M. J. P. Mandigma⁺
 School of Chemistry, University of Bristol, Cantock's Close, Bristol,
 BS8 1TS, United Kingdom

J. P. Barham
 Department of Pure & Applied Chemistry, University of Strathclyde,
 Glasgow, G1 1XL, United Kingdom

[†] These authors contributed equally.

© 2025 The Author(s). Angewandte Chemie International Edition published by Wiley-VCH GmbH. This is an open access article under the terms of the Creative Commons Attribution License, which permits use, distribution and reproduction in any medium, provided the original work is properly cited.

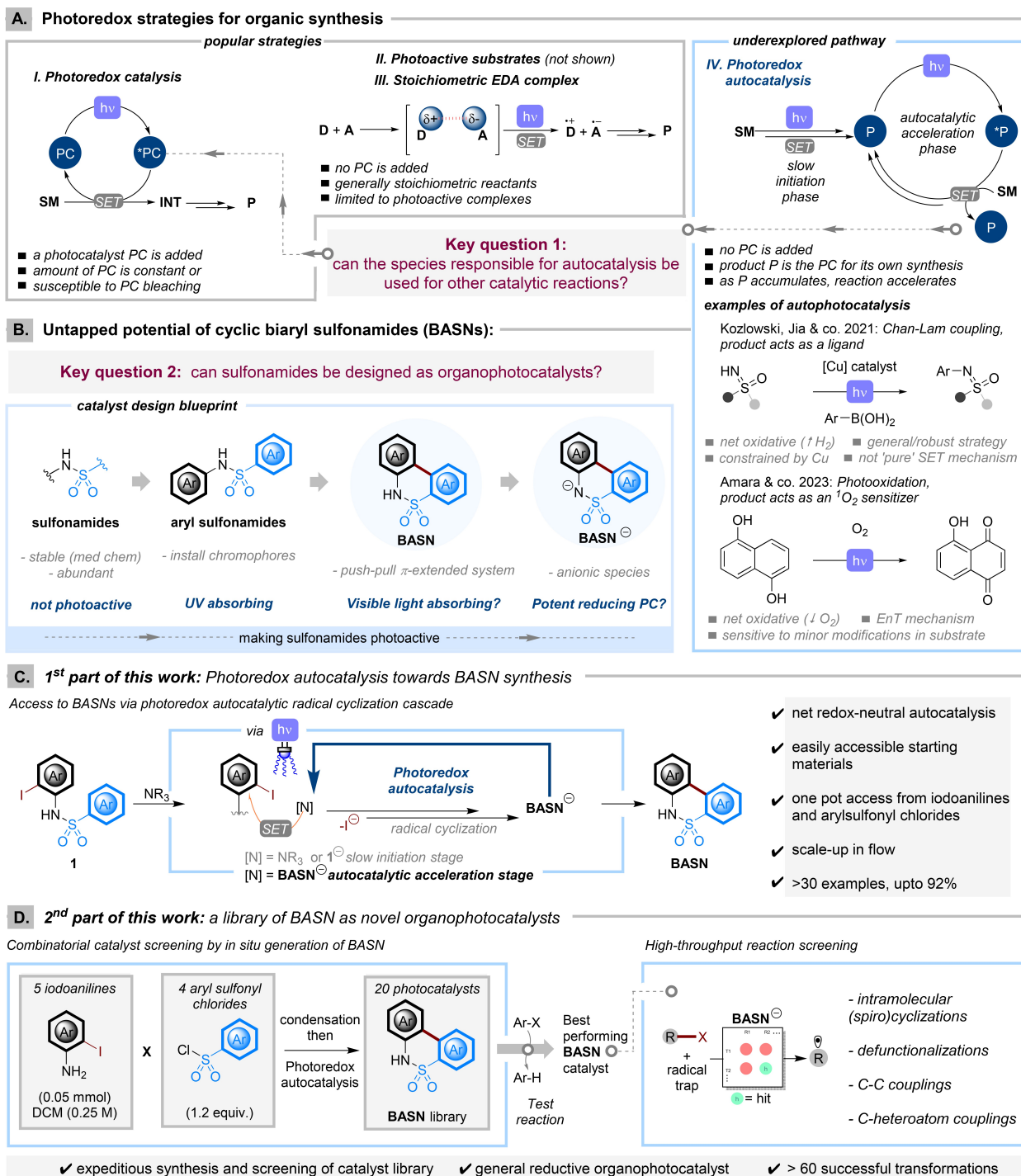


Figure 1. Key concepts in photochemistry. (A) Photoredox mechanisms. (B) Photocatalytic potential of sulfonamides. (C) Photoredox autocatalytic access of BASN. (D) Self-synthesizing library concept allowing reaction screening of BASNs as exogenous photocatalysts.

dented as its reactivity mainly involves the applications of *N*-centered radicals (i.e. as hydrogen atom transfer (HAT) agents).^[13] Nevertheless, the ease of sulfonamide anion oxidation is an attractive starting point for a catalyst design.^[14] Intuitively, incorporating aryl groups at the sulfonamide's nitrogen and sulfonyl positions—i.e. a cyclic biaryl sulfonamide (BASN)—could make the compound photoactive and shift absorption to the visible region by

setting up a push-pull extended π electronic system (Figure 1B, left). With this catalyst design at hand and considering that BASNs themselves are emerging bioactive compounds, we sought to investigate the synthetic and catalytic potential of BASNs.

In this study, we report a photoredox autocatalytic pathway towards BASN, implying that if BASN can act as a photocatalyst for its own formation, it could also catalyze

other reactions. Exploiting the ease of synthesis of BASN, a rapid combinatorial design allowed one-pot, in situ generation of diverse BASN photocatalysts from inexpensive, and easily accessible building blocks. This photocatalyst library was then directly screened in photo-reductive transformations and as such this design enabled rapid identification of the optimal photocatalyst structure.

Results and Discussion

Reaction Development

With cost and synthetic ease in mind, we envisaged synthesizing BASNs (**2a** and **2b**) starting with a simple condensation of readily accessible iodoanilines with aryl sulfonyl chlorides, followed by a radical cyclization (Figure S3 for retrosynthesis and cost analysis). At the onset of the study, we investigated the reductive radical cyclization of tosylated *o*-iodoaniline **1a** induced by SET reduction of the aryl iodide by a radical anionic organophotocatalyst, the latter itself generated by photoexcitation in the presence of an amine donor (Figure 2A). Catalytic loadings of 4CzIPN or NpMI gave BASN product **2a** in 52 % and 50 % respectively. However, we were surprised that the reaction worked even without a photocatalyst—affording **2a** in 34 %. Even more so, the yield of **2a** improved (to 40 %) by irradiation of the reaction mixture containing only **1a** and tributylamine (i.e., in the absence of a photocatalyst and an inorganic base). After design of experiment (DoE) optimization and further screening of conditions (see SI, Section 5.2 full details), we identified that the use of *N,N*-dimethylethanolamine (DMEA) and blue light irradiation ($h\nu=450\text{ nm}$) afforded **2a** in a high yield (84 %) within a short reaction time of 3 h. Furthermore, fluorine-containing BASN **2b** was accessed in excellent yield (91 %) under these conditions. Control reactions confirmed that both light and DMEA are crucial for this transformation.

Mechanistic Investigations: Discovery of Photoredox Autocatalysis

Intrigued by the efficiency of this reaction and the fact that exogenous photocatalyst was not required, the mechanism was then probed. The reaction profile for the consumption of **1b** / formation of **2b** (monitored using ^{19}F NMR) displayed a sigmoidal curve (Figure 2C) whose second derivative revealed a parabolic shape (Figure S21). This establishes that the reaction has three phases: slow initiation, acceleration (with the maximum rate reached when $[\mathbf{1b}] = [\mathbf{2b}]$), and a saturation phase—hallmarks of an autocatalytic process.^[4,5,15] To check this, we performed the unequivocal test for autocatalysis, which involves the effect of adding product on the initial rates.^[5] Therefore, **2a** was added at increasing catalytic loadings: 0 mol %, 10 mol %, and 20 mol % (Figure 2D). Indeed, the initial rate for the formation of **2b** (i.e., slope of the yield as a function of time) increases as the loading of BASN **2a**. UV/Vis spectroscopy

and spectroelectrochemistry (see SI, Section 6.7) revealed that the deprotonated product is the light absorbing species at the blue region - tailing until ca. 450 nm - catching the tail end of the emission of the 450 nm LED employed (Figure 2B). ^1H NMR studies confirmed that the sulfonamide moieties of **1** and **2** are deprotonated under the reaction conditions, consistent with the matched pKas of arylsulfonamides (pKa of **1a**=8.1 and pKa of **2a**=8.9,^[16] and DMEA (pKaH=9.23).^[17] Taken together, we propose that deprotonated **2** is the active photocatalyst in its own autocatalytic synthesis that engages **1** in electron transfer. Consistent with this proposal, testing an *N*-methylated sulfonamide - that cannot be deprotonated - afforded **3a** (see below) only in trace amounts. Repeating the same reaction by adding a catalytic amount of **2a** considerably increased the yield of **3a** to 48 % (Figure S22).

Considering the electron rich nature of the aryl iodide of deprotonated **1**, we propose it undergoes a concerted dissociative SET reduction (bypassing a radical dianion intermediate) following the Marcus Savéant theory, directly affording the aryl radical intermediate.^[18] Density Functional Theory (DFT) calculations revealed that the most suitable SET donor present would be the deprotonated product BASN⁻ (See SI, Section 6.14). Time Dependent Density Functional Theory (TD-DFT) analysis of BASN⁻'s longest wavelength excitation revealed a $\pi\rightarrow\pi^*$ transition involving charge transfer from the electron rich aniline moiety (especially localized on its anionic N atom) across the entire electron poor biaryl moiety (Figure 2E); such a charge transfer is reminiscent of a typical organophotocatalyst excitation.^[19]

From the UV/Vis, cyclic voltammetry (CV), and emission experiments, it was estimated that *BASNs **2a**⁻ and **2b**⁻ can reach excited state redox potentials of approximately -2.45 V and -2.31 V versus SCE, respectively^[20] (Figure S19). Although a very low measured quantum yield (<0.5 %) suggests a radical chain mechanism is unlikely (e.g. a base-promoted homolytic aromatic substitution pathway),^[21] it cannot be completely ruled out. From these experiments, we propose the following photoredox autocatalytic cycle (Figure 2F). After deprotonation of the starting material **i**, a mildly photo-absorbing anionic intermediate **i**⁻ is excited by light. A concerted dissociative SET - either from DMEA (to ***i**⁻) or to another equivalent of **i**⁻ (from ***i**⁻) - generates aryl radical intermediate **ii**, followed by dearomative *ortho*-cyclization to form **iii**. Rearomatization by SET and deprotonation (or by HAT) affords a deprotonated BASN⁻ product, marking the end of a slow initiation phase. Once the BASN⁻ is present in the system, this acts as a photoredox autocatalyst for a redox-neutral cyclization of another equivalent of **i**⁻, intercepting the catalytic cycle again after aryl radical generation and re-aromatization. This photoredox autocatalytic phase is faster as i) BASN⁻ has the most efficient absorption at the blue region, ii) packs the highest reductive redox power in its excited state, and iii) the photocatalyst concentration increases with every turnover.

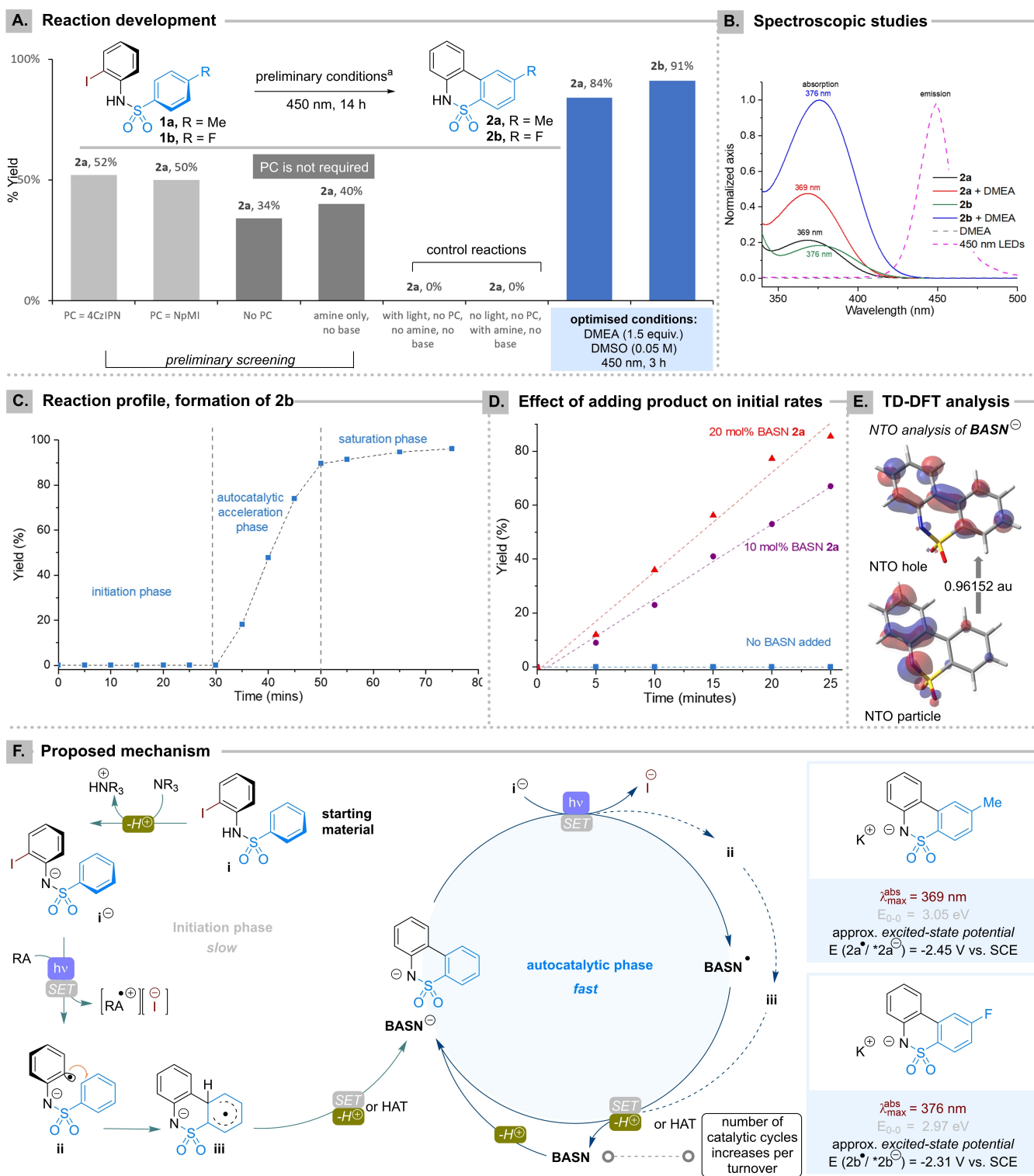


Figure 2. Reaction development and mechanistic studies. (A) Preliminary reaction screening and optimized conditions. (B) UV-Vis spectra of BASN **2a** and **2b** and their deprotonated counterparts. (C) Kinetic profile for the formation of **2b**. (D) Effect of adding BASN **2a** to the initial rate for the formation of **2b**. (E) TD-DFT for NTO analysis of BASN. (F) Proposed photoredox autocatalytic mechanism. ^a K_2HPO_4 (2 equiv.), amine = NBu_3 (2 equiv.), PC (5 mol%), DMSO:H₂O (9:1), RA = reducing agent.

Substrate Scope

After the photoredox autocatalytic nature of the reaction was established, the scope of self-synthesizing BASNs was examined (Figure 3). We were delighted to find generally high yields (up to 92%) across a broad library of (photocatalyst) structures (34 examples); varying the electronics and positions of substituents on both the aryl sulfonyl group

(**2a** to **2p**) and the aminoaryl group (**2q** to **2ad**). Exceptions were present such as **2h** and **2o** which were afforded in relatively low yields as *ortho*-substituents on the aryl sulfonyl side could promote a Smiles-Truce rearrangement.^[22] Substrates bearing aryl sulfonyls which are too electron poor or with extended conjugation were not well-tolerated. Either desulfonation (**1ai** to **1ak**) or no reaction (**1al**) occurred. Moreover, replacement of iodide

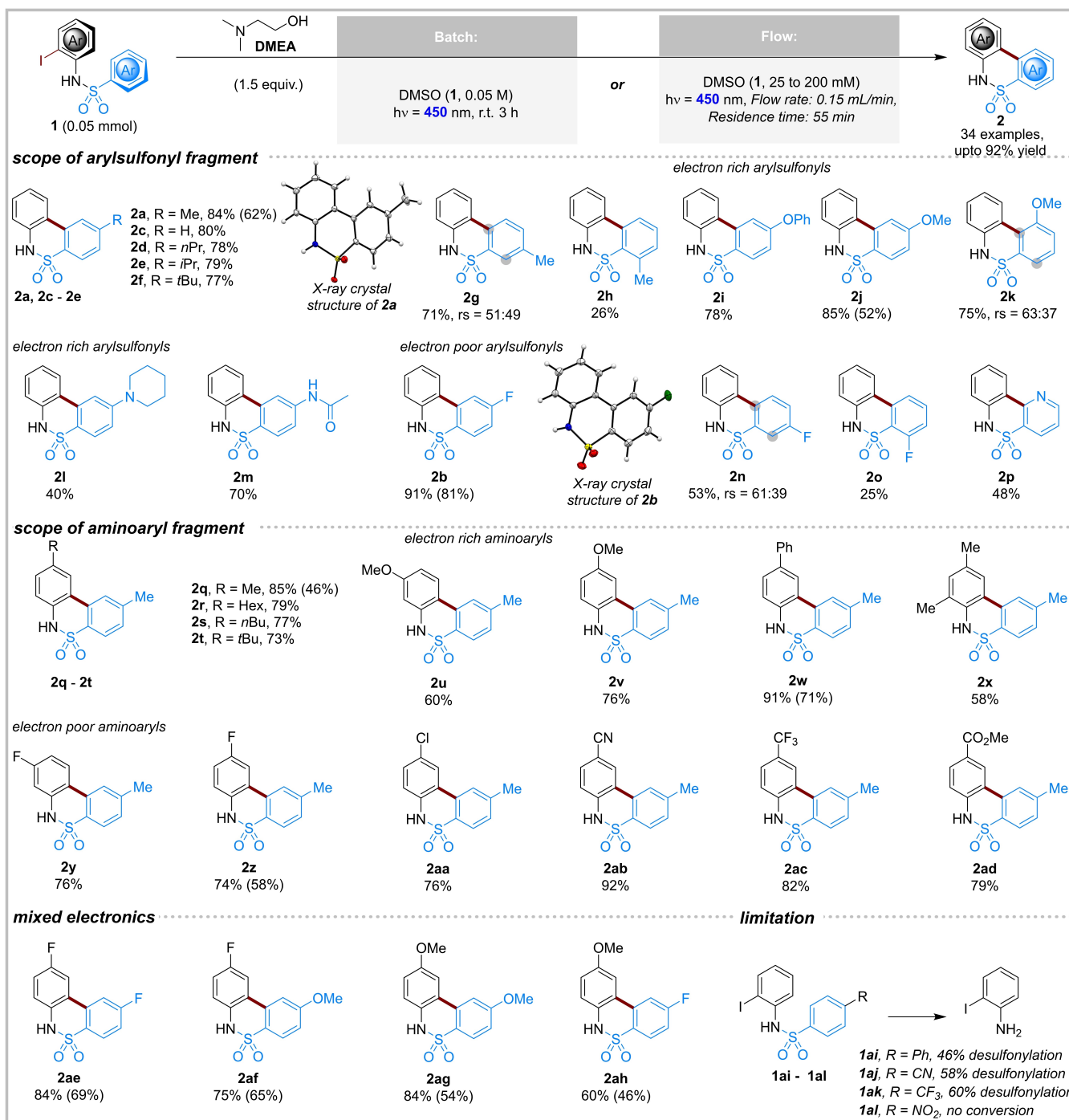


Figure 3. Substrate scope of photoredox autocatalytic BASN synthesis. ^aYields obtained with flow are inside the parenthesis (Table S14 and Figure S32). rs = regioselectivity ratio where the regio-isomer connectivity is indicated by the grey circle with the major isomer as drawn.

with bromide in **1a** resulted in detosylation (80%). Representative examples (**2a**, **2b**, **2j**, **2q**, **2w**, **2z**, **2ae**, **2af**, **2ag**, and **2ah**) were accessed on a semi-preparative scale using a commercially available photo-flow reactor without optimization in moderate to high yields (Figure 3, yields in parenthesis).

To further challenge the practicality of this method, we examined its scalability, the use of direct sunlight, and the plausibility of a one-pot BASN synthesis from commercial materials (Figure 4). Gram scale (10 mmol) synthesis of **2b** was achieved in flow, affording a high yield (81%) and decent productivity (3 g/day) without the need of chromatography for purification. To our delight, we were able to harness energy from sunlight on a fair day for a 5 mmol preparative scale synthesis of **2a**, achieving a good yield (65%). Finally, we showcased a telescoped synthesis of **2a** directly from commercially-available *o*-iodoaniline **4** and tosyl chloride **5** without much erosion of yield (73%) compared to the single-step process.

Combinatorial Approach towards the Library Synthesis of BASN Photocatalysts

Considering BASN⁻'s photophysical and reductive properties (see above), we investigated its use as a photocatalyst. We chose reductive defunctionalizations of aryl halides - methyl 2-chlorobenzoate (-2.00 V vs SCE) and 4-bromobiphenyl (-2.4 V vs SCE) - as model reactions. Taking advantage of the successful telescoped synthesis of BASN and to expedite determination of the best BASN structure for reductive defunctionalizations, a combinatorial catalyst screening approach was designed whereby nine building blocks (i.e., five sulfonyl chlorides and four iodoanilines) were used to assemble a 4×5 library of 20 BASN structures in parallel by telescoped sulfonamide synthesis and photoredox autocatalytic cyclization (Figure 5A). Subsequently, the reductive defunctionalization of aryl halides was tested

against these *in situ* generated photocatalysts (Figure 5B). While all 20 catalyst structures performed well with the activated aryl chloride substrate (yields ranging from 81% to >99%, Figure S34), the variation in catalytic performance was more pronounced when model substrate 4-bromobiphenyl was used which has a deeper reduction potential (Figure 5B). Here, the best performing photocatalyst is BASN **2b**. We recognize that the efficiencies of the photoredox autocatalytic step might differ between catalysts, leading to different final catalyst concentrations. However, the reductive defunctionalization reaction was fairly insensitive to catalyst loading as the yield of debromination does not correlate with the amount of the catalyst present ($R^2=0.0519$, Figure S36). Furthermore, a confirmatory experiment affording 77% of the biphenyl product using 10 mol% of BASN **2b** is at par with the result from the library screening. A control experiment employing *N*-phenyl-*p*-toluenesulfonamide as a catalyst did not yield dehalogenated product, confirming the cyclic biaryl scaffold is important for the photocatalytic performance.

Benchmarking experiments against Mes-Acr⁺ BF₄⁻, 3DPA2FBN, and PDI photocatalysts (20–55% yields of biphenyl) demonstrated that the dehalogenation of 4-bromobiphenyl using BASN **2b** achieves the highest yield (75%) after 6 hours under mild visible light irradiation (see Supporting Information file, Section 10, for detailed benchmarking studies).

After identifying BASN **2b** as the best photocatalyst, it was used for the synthesis of several other heterocyclic structures (whose products or intermediates are incapable of autocatalysis), exploiting the generation of aryl radicals from aryl iodides followed by intramolecular cyclization (Figure 6). Examples include six-membered *N*-methylated biaryl sultams (**3a** and **3b**), and biaryl sultones (**3c** to **3e**). Keeping in mind pharmaceutically-relevant ring systems, we synthesized novel seven-membered cyclic biaryl variants (**3f** to **3i**) and assembled spirocyclic structures via a cascade of aryl radical generation followed by 1,5-HAT and then

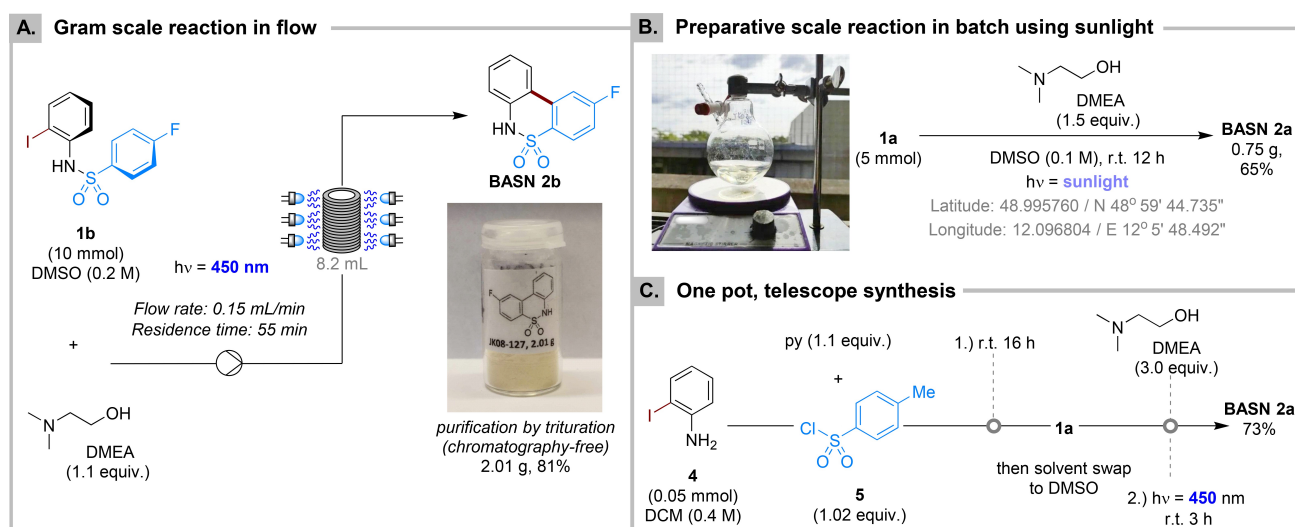


Figure 4. BASN synthesis. (A) scale-up in flow. (B) sunlight irradiation in batch. (C) telescoped synthesis. py=pyridine.

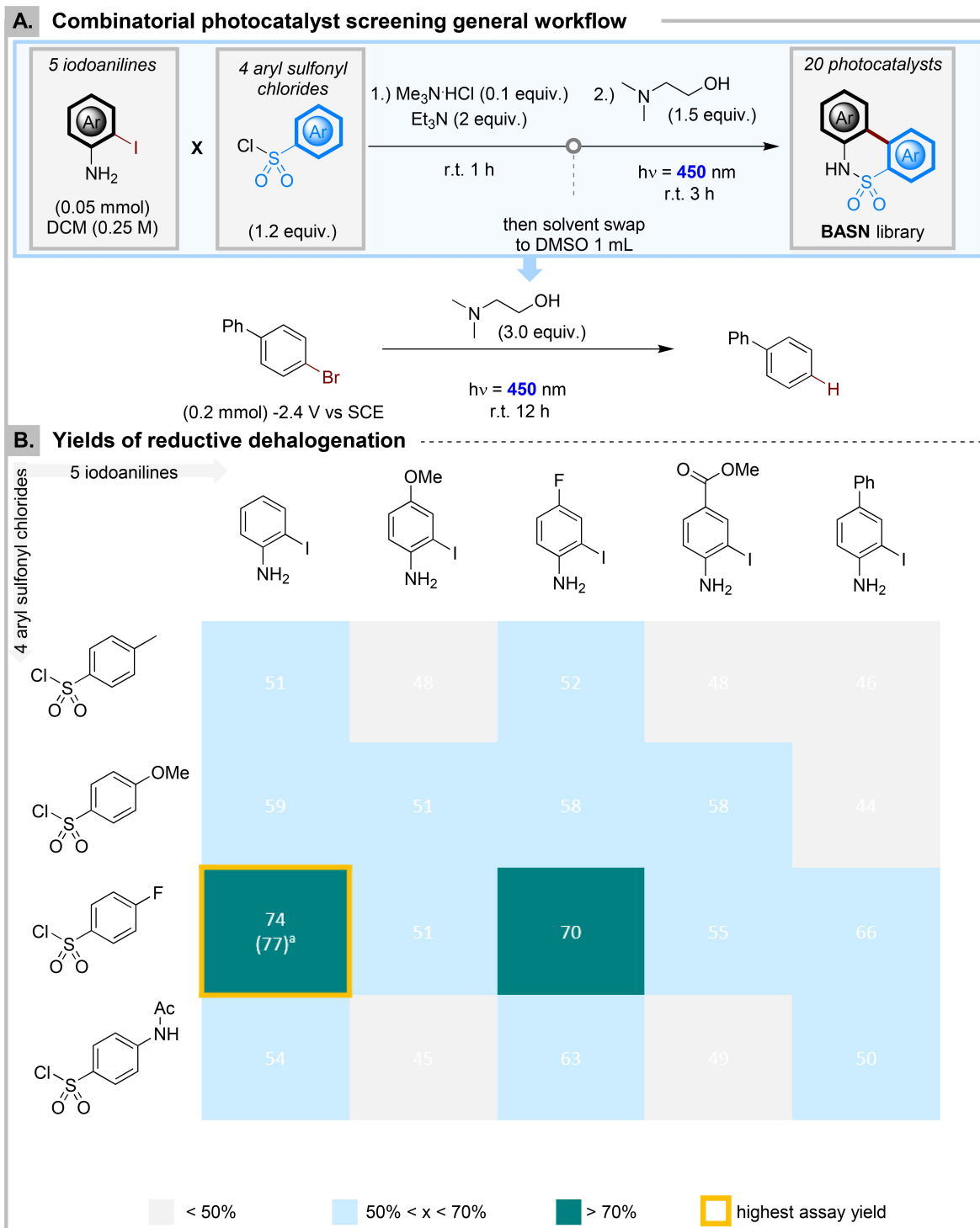


Figure 5. Combinatorial catalyst screening. (A) In situ generation of 20 different BASN structures. (B) Reductive dehalogenation using in situ formed BASN photocatalysts. py = pyridine. ^aconfirmatory experiment using 10 mol % of BASN **2b**.

radical cyclization (**6a** to **6k**). In the reaction forming **6c**, BASN **2b** recovery after the reaction was 100 % (¹H NMR). To further investigate the generality of BASN as a reductive organophotocatalyst, a high throughput reaction screening^[23] was conducted (Figure S37 and Table S15). Good hits for reductive activation were obtained for a selection of radical

precursors including aryl halides, a benzoate ester, an *N*-(acyloxy)phthalimide (NHPI) esters, a Katritzky salt, Togni's reagent II (**Tr-II**), and an aryl sulfonium salt (Figure 7A).

Figure 7B outlines examples for reductive defunctionalizations such as dehalogenations of aryl chlorides, bromides,

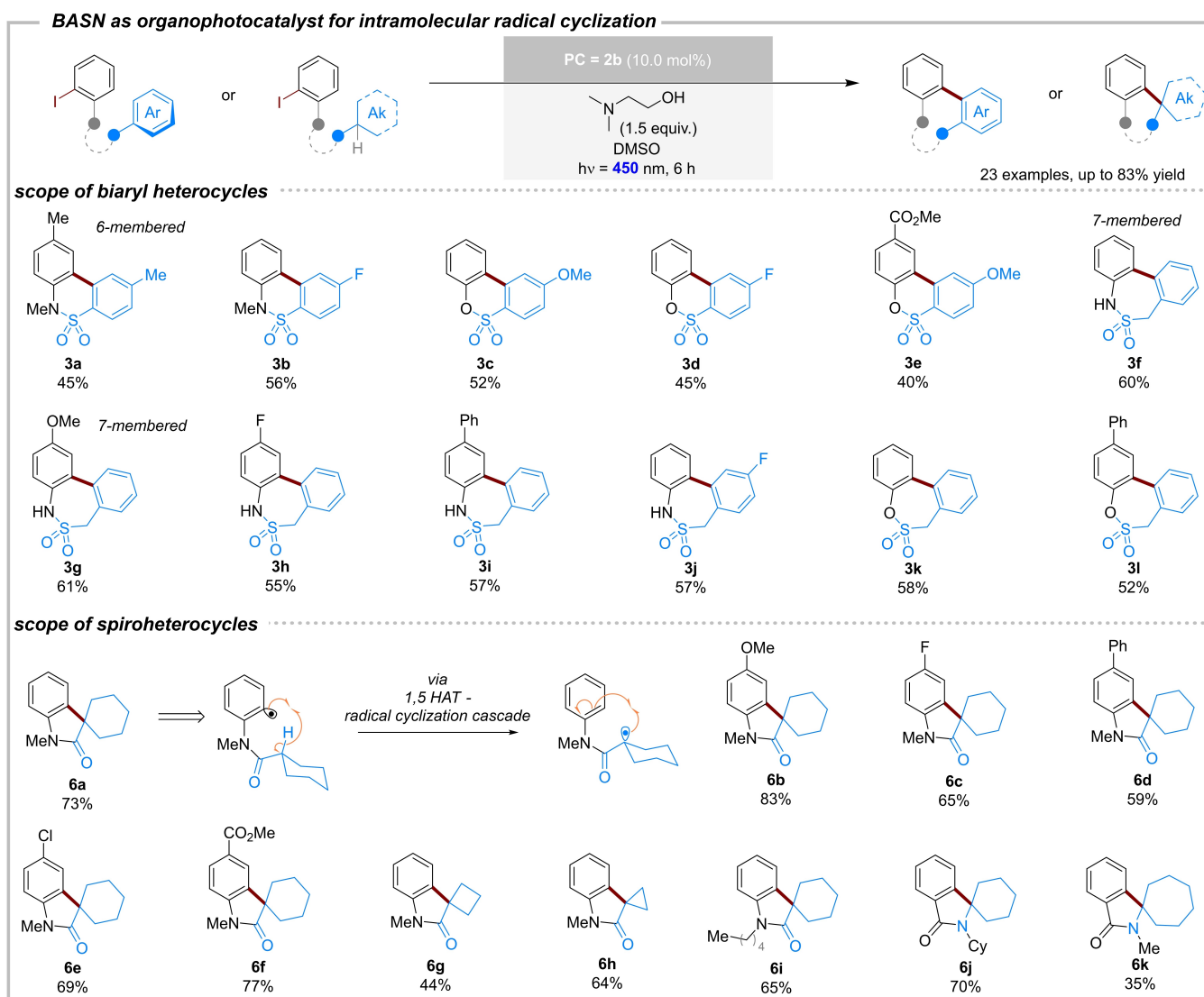


Figure 6. BASN 2b as a reductive organophotocatalyst. Synthesis of heterocycles via visible light-promoted radical cyclizations catalyzed by BASN 2b.

and iodides (**7a** to **7c**), desotylations (**7e** and **7f**), and deoxygenations of trifluoromethylated benzoate esters (**7g** and **7h**). In the desotylation of **7e**, BASN **2a** (72% yield of aniline after 6 h) outperformed other organophotocatalysts tested (PDI, Mes-Acr⁺ BF₄⁻ and 3DPA2FBN; 24–34% yields after 6 h). Recovery of BASN **2a** was 82% (¹H NMR), which was surprising that a catalyst containing a tosyl-like group would persist in a desotylation reaction. We assume that upon reductive N–S cleavage the biaryl linker holds the anilide N anion and sulfonyl radical in close proximity for catalyst repair via recombination. Together with the quantitative recovery of BASN **2b** in the reaction forming **6c**, this contrasts with 3DPA2FBN, recovered in < 2% in both cases.

Next, we turned our attention to complexity-building reactions such as transition metal-free C–C couplings of alkyl, aryl and trifluoromethyl radical precursors with olefins or heterocycles (Figure 7C) affording various Csp³–Csp² or

Csp²–Csp² linkages (**8a** to **8o**). Interestingly, removing the base gave better yields with NHPI esters (**8a** to **8i**) which could be attributed to a favorable catalyst-substrate pre-assembly via synergistic H-bond and π -stacking that assisted a photoinduced intra-complex electron transfer (Figure 7C.1, Figure S40 for the yields with base, and Section 6.14 for computational investigations).^[24] Activation and C-heteroatom coupling of aryl chlorides was also demonstrated (Figure 7D) obtaining phosphorylation (**9a** to **9k**), borylation (**9l** and **9m**), and sulfidation (**9n** and **9o**) products. Late-stage diversification of industrially-relevant molecules (gemfibrozil \rightarrow **8h** and **8j**, caffeine \rightarrow **8o**, boscalid \rightarrow **9k**, and menthol \rightarrow **9m**) and introduction of benzene bioisosteres bicyclo[1.1.1]pentane (**8g**) and bicyclo[2.2.2]octane (**8f** and **8i**) were demonstrated, further highlighting the synthetic utility of this method. Photophysical characterization of deprotonated BASNs **2a** and **2b** found lifetimes of the order 5–7 ns, which were quenched by **7c** and the

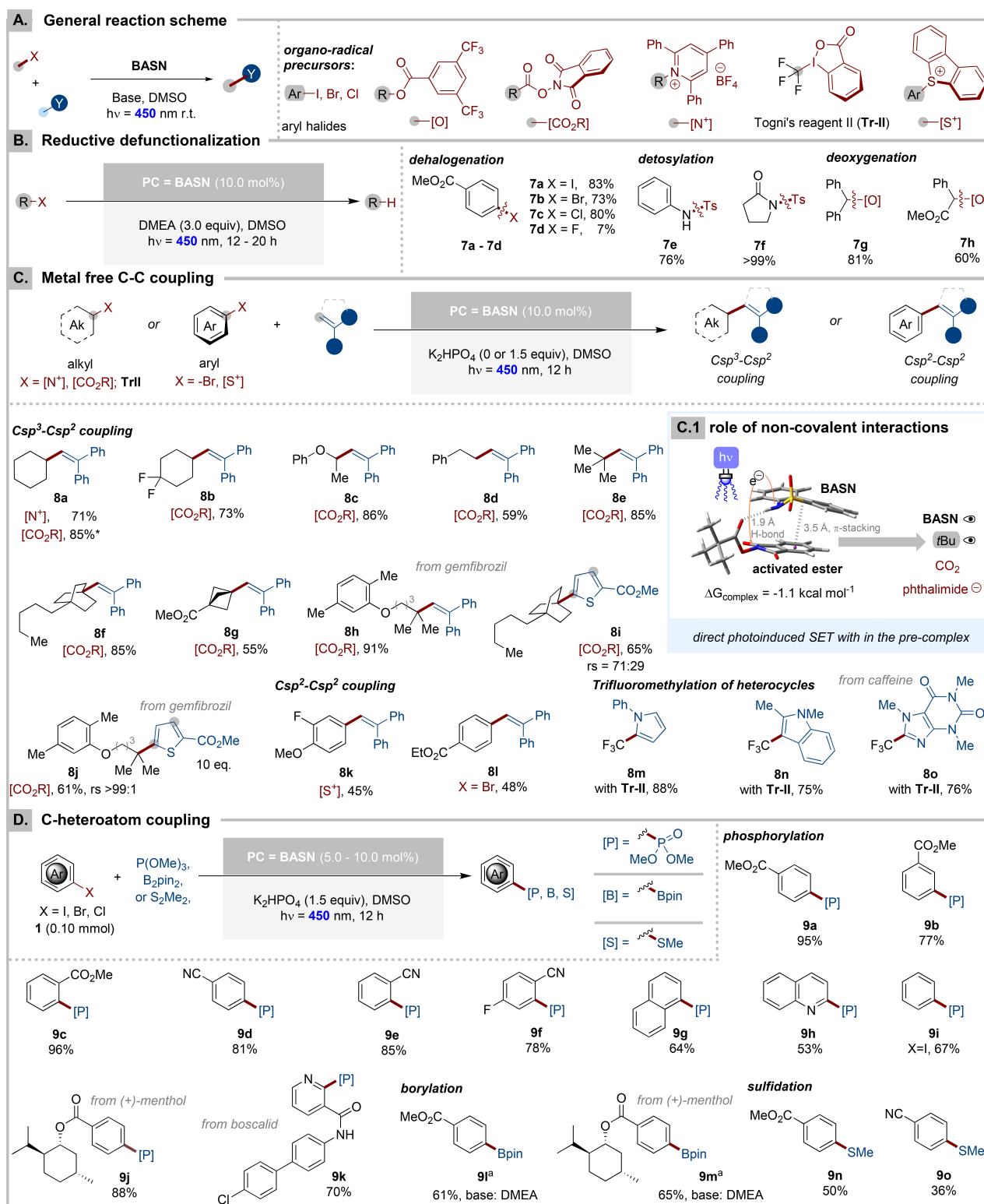


Figure 7. BASN as an organophotocatalyst. Applications in reductive defunctionalizations, transition metal-free Csp³-Csp² couplings, Csp²-Csp² couplings, trifluoromethylation of heterocycles and Csp²-heteroatom couplings. ^aDMEA used as the base.

NHPI ester of cyclohexanecarboxylic acid (see SI, Sections 6.3–6.5 for steady-state and time-resolved emission experiments) with rate constants of ($k_q =$) $\sim 5 \times 10^9 \text{ M}^{-1} \text{ s}^{-1}$.

Conclusions

In conclusion, this study outlines the systematic exploration of photoredox autocatalysis to access cyclic biaryl sulfona-

mides (BASNs). This approach facilitated the development of BASNs as novel, widely applicable reductive organophotocatalysts, which are easily diversifiable and efficiently accessible in a low-cost, one-pot process from iodoanilines and sulfonyl chlorides. Given the ubiquity of these precursors and the prominent role of sulfonamides and biaryls as robust, biocompatible motifs in medicinal chemistry, we anticipate this class of photocatalyst will be of significance to both industry and academia. Additionally, it may pave the way for further biological applications of BASNs. We envisage that this study on photoredox autocatalysis will contribute to the advancement of the budding field of autophotocatalysis.

Supporting Information

The authors have cited additional references within the Supporting Information [25–100].

Acknowledgements

JK, MJPM and JPB thank the Alexander von Humboldt Foundation for funding, provided within the framework of the Sofja Kovalevskaja Award endowed to JPB by the German Federal Ministry of Education and Research. JK is co-financed by a BDF (Bayerischen Gleichstellungsförderung) Scholarship for which she thanks the Bayerische Staatsministerium für Wissenschaft und Kunst. NAB thanks the German Academic Exchange Service (DAAD) for a DAAD-WISE scholarship for NAB's research exchange to Universität Regensburg. JK and JPB are members of DFG TRR 325 'Assembly Controlled Chemical Photocatalysis' (444632635) and thank other members of the TRR for insightful discussions. We thank Regina Hoheisel for measuring cyclic voltammetry, Julia Zach and Wolfgang Haumer for assistance and training in luminescence spectroscopy measurements, Julia Zach for assistance and training in quantum yield and lifetime measurements, Birgit Hischa for running X-ray diffraction analyses, Fritz Kastner and Tuan Anh Nguyen for measuring NMR samples with Bruker 600 MHz, and Dr. Rudolf Vasold for measuring GC-MS samples of high-throughput screening reactions. We thank Mr. Simon Schmid for providing the German translated manuscript. Open Access funding enabled and organized by Projekt DEAL.

Conflict of Interest

The authors declare no conflict of interest.

Data Availability Statement

The data that support the findings of this study are available in the supplementary material of this article.

Keywords: Autocatalysis · Combinatorial Library · Sulfonamides · Flow Chemistry · Photocatalysis

- [1] a) H. E. Bonfield, T. Knauber, F. Lévesque, E. G. Moschetta, F. Susanne, L. J. Edwards, *Nat. Commun.* **2020**, *11*, 804; b) G. Ciamician, *Science* **1912**, *36*, 385; c) C. K. Prier, D. A. Rankic, D. W. C. MacMillan, *Chem. Rev.* **2013**, *113*, 5322; d) D. M. Schultz, T. P. Yoon, *Science* **2014**, *343*, 1239176; e) C. Stephenson, T. Yoon, *Acc. Chem. Res.* **2016**, *49*, 2059.
- [2] a) *Visible Light Photocatalysis in Organic Chemistry* (Eds.: C. R. J. Stephenson, T. P. Yoon, D. W. C. MacMillan), Wiley-VCH Verlag GmbH & Co, Weinheim, Germany, **2018**; b) J. Twilton, C. Le, P. Zhang, M. H. Shaw, R. W. Evans, D. W. C. MacMillan, *Nat. Chem. Rev.* **2017**, *1*, 1.
- [3] a) G. E. M. Crisenza, D. Mazzarella, P. Melchiorre, *J. Am. Chem. Soc.* **2020**, *142*, 5461; b) R. Foster, *J. Phys. Chem.* **1980**, *84*, 2135; c) S. V. Rosokha, J. K. Kochi, *Acc. Chem. Res.* **2008**, *41*, 641.
- [4] A. J. Bissette, S. P. Fletcher, *Angew. Chem., Int. Ed.* **2013**, *52*, 12800.
- [5] A. K. Horváth, *Phys. Chem. Chem. Phys.* **2021**, *23*, 7178.
- [6] a) D. G. Blackmond, *Angew. Chem., Int. Ed.* **2009**, *48*, 386; b) M. ter Harmsel, O. R. Maguire, S. A. Runikhina, A. S. Y. Wong, W. T. S. Huck, S. R. Harutyunyan, *Nature* **2023**, *621*, 87; c) M. G. Howlett, S. P. Fletcher, *Nat. Chem. Rev.* **2023**, *7*, 673; d) M. Avalos, R. Babiano, P. Cintas, J. L. Jiménez, J. C. Palacios, *Chem. Commun.* **2000**, 887; e) T. A. Lincoln, G. F. Joyce, *Science* **2009**, *323*, 1229.
- [7] a) S. V. Athavale, A. Simon, K. N. Houk, S. E. Denmark, *Nat. Chem.* **2020**, *12*, 412; b) K. Soai, T. Kawasaki, A. Matsumoto, *Chapter 1. Asymmetric Autocatalysis: The Soai Reaction, an Overview*, **2022**; c) K. Soai, T. Shibata, H. Morioka, K. Choi, *Nature* **1995**, *378*, 767; d) D. G. Blackmond, C. R. MacMillan, S. Ramdeehul, A. Schorm, J. M. Brown, *J. Am. Chem. Soc.* **2001**, *123*, 10103; e) N. Chinkov, A. Warm, E. M. Carreira, *Angew. Chem., Int. Ed.* **2011**, *50*, 2957.
- [8] a) S. N. Semenov, L. Belding, B. J. Cafferty, M. P. S. Mousavi, A. M. Finogenova, R. S. Cruz, E. V. Skorb, G. M. Whitesides, *J. Am. Chem. Soc.* **2018**, *140*, 10221; b) B. Wang, I. O. Sutherland, *Chem. Commun.* **1997**, 1495; c) K. J. Singh, A. C. Hoepker, D. B. Collum, *J. Am. Chem. Soc.* **2008**, *130*, 18008; d) M. Malakoutikhah, J. J.-P. Peyralans, M. Colomb-Delsuc, H. Fanlo-Virgós, M. C. A. Stuart, S. Otto, *J. Am. Chem. Soc.* **2013**, *135*, 18406; e) W. Cullen, A. J. Metherell, A. B. Wragg, C. G. P. Taylor, N. H. Williams, M. D. Ward, *J. Am. Chem. Soc.* **2018**, *140*, 2821.
- [9] C. Wang, H. Zhang, L. A. Wells, T. Liu, T. Meng, Q. Liu, P. J. Walsh, M. C. Kozłowski, T. Jia, *Nat. Commun.* **2021**, *12*, 932.
- [10] a) S. Kim, A. Martínez Dibildox, A. Aguirre-Soto, H. D. Sikes, *J. Am. Chem. Soc.* **2021**, *143*, 11544; b) S. Kim, H. D. Sikes, *ACS Appl. Mater. Interfaces* **2021**, *13*, 57962.
- [11] M. Lancel, P. Zimmerlin, C. Gomez, M. Port, L. Khrouz, C. Monnereau, Z. Amara, *J. Org. Chem.* **2023**, *88*, 6498.
- [12] N. A. Romero, D. A. Nicewicz, *Chem. Rev.* **2016**, *116*, 10075.
- [13] a) K. Kwon, R. T. Simons, M. Nandakumar, J. L. Roizen, *Chem. Rev.* **2022**, *122*, 2353; b) K. Ram Bajya, M. Kumar, A. Ansari, S. Selvakumar, *Adv. Synth. Catal.* **2023**, *365*, 976; c) N. Tang, X. Wu, C. Zhu, *Chem. Sci.* **2019**, *10*, 6915; d) C. Pratley, S. Fenner, J. A. Murphy, *Chem. Rev.* **2022**, *122*, 8181; e) H. Tanaka, K. Sakai, A. Kawamura, K. Oisaki, M. Kanai, *Chem. Commun.* **2018**, *54*, 3215; f) X. Teng, T. Yu, J. Shi, H. Huang, R. Wang, W. Peng, K. Sun, S. Yang, X. Wang, *Adv. Synth. Catal.* **2023**, *365*, 3211.
- [14] M. Schmalzbauer, M. Marcon, B. König, *Angew. Chem., Int. Ed.* **2021**, *60*, 6270.

- [15] A. I. Hanopolskyi, V. A. Smaliak, A. I. Novichkov, S. N. Semenov, *ChemSystemsChem* **2021**, *3*, e2000026.
- [16] X. Pan, H. Wang, C. Li, J. Z. H. Zhang, C. Ji, *J. Chem. Inf. Model.* **2021**, *61*, 3159.
- [17] R. J. Littel, M. Bos, G. J. Knoop, *J. Chem. Eng. Data* **1990**, *35*, 276.
- [18] a) C. Costentin, M. Robert, J.-M. Savéant, *Chem. Phys.* **2006**, *324*, 40; b) L. Pause, M. Robert, J.-M. Savéant, *J. Am. Chem. Soc.* **1999**, *121*, 7158; c) J. M. Saveant, *J. Am. Chem. Soc.* **1987**, *109*, 6788.
- [19] M. J. P. Mandigma, J. Kaur, J. P. Barham, *ChemCatChem* **2023**, *15*.
- [20] S. Wu, F. Schiel, P. Melchiorre, *Angew. Chem., Int. Ed.* **2023**, *62*, e202306364.
- [21] a) A. Studer, D. P. Curran, *Angew. Chem., Int. Ed.* **2011**, *50*, 5018–5022; b) J. P. Barham, G. Coulthard, K. J. Emery, E. Doni, F. Cumine, G. Nocera, M. P. John, L. E. A. Berlouis, T. McGuire, T. Tuttle, J. A. Murphy, *J. Am. Chem. Soc.* **2016**, *138*, 7402–7410.
- [22] a) T. Sephton, J. M. Large, L. Natrajan, S. Butterworth, M. F. Greaney, *Angew. Chem., Int. Ed.* **2024**, e202407979; b) C. Hervieu, M. S. Kirillova, T. Suárez, M. Müller, E. Merino, C. Nevado, *Nat. Chem.* **2021**, *13*, 327.
- [23] F. Strieth-Kalthoff, C. Henkel, M. Teders, A. Kahnt, W. Knolle, A. Gómez-Suárez, K. Dirian, W. Alex, K. Bergander, C. G. Daniliuc, B. Abel, D. M. Guldi, F. Glorius, *Chem* **2019**, *5*, 2183.
- [24] a) S. Wu, J. Žurauskas, M. Domański, P. S. Hitzfeld, V. Butera, D. J. Scott, J. Rehbein, A. Kumar, E. Thyrhaug, J. Hauer, J. P. Barham, *Org. Chem. Front.* **2021**, *8*, 1132–1142; b) X. Tian, T. A. Karl, S. Reiter, S. Yakubov, R. de Vivie-Riedle, B. König, J. P. Barham, *Angew. Chem., Int. Ed.* **2021**, *60*, 20817–20825; c) L. Wylie, J. P. Barham, B. Kirchner, *ChemPhysChem* **2023**, *24*, e202300470.

Manuscript received: November 27, 2024

Accepted manuscript online: February 18, 2025

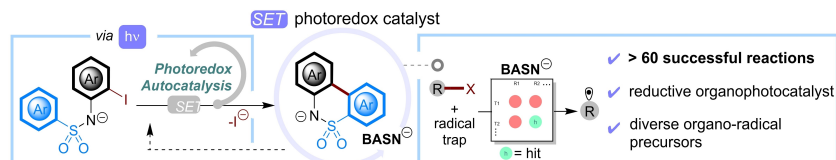
Version of record online: ■■■, ■■■

Research Article

Photochemistry

J. Kaur, M. J. P. Mandigma, N. A. Bapat,
J. P. Barham* e202423190

Photoredox Autocatalysis: Towards a Library of Generally Applicable Sulfonamide Reductive Photocatalysts



Photoredox autocatalysis is revealed to access cyclic biaryl sulfonamides (BASNs) without an initial exogenous photocatalyst. While unveiling photoredox autocatalysis is important to the enrichment of basic research, this has

also led to further practical applications such as rapid discovery of novel, potent and readily accessible photocatalyst scaffolds, BASNs, which catalyze manifolds of meaningful transformations.